

M.A.Omar¹,
N.Abdullah¹,
R.Sayuti¹,
F. Ismail¹,
N.Zainon¹, and
Baharuddin,
M.Y.²

¹Advanced Materials Research Centre (AMREC), SIRIM
Berhad, Lot 34, Jalan Hi Tech 2/3, Kulim Hi Tech Park,
09000 Kulim, Kedah

²Faculty of Allied Health, Cyberjaya University College of
Medical Sciences
63000 Cyberjaya, Selangor

*(afian@sirim.my)

STUDY OF FEEDSTOCK PREPARATION AND DEBINDING PROCESS OF INJECTION MOULDED HIP STEM Co-Cr-Mo ALLOY POWDER USING WAX-BASED BINDER

RINGKASAN: Pengacuan suntikan logam (MIM) telah mengalami berbagai kemajuan di dalam pembangunan sistem pengikat dimana objektifnya adalah untuk mengurangkan masa, semasa proses penyahikatan. Di dalam kerja penyelidikan ini, sistem pengikat bahan lilin telah digunakan didalam penghasilan 'hip stem' dengan menggunakan serbuk logam CoCrMo dengan purata saiz serbuk logam adalah 16 μm dengan menggunakan sistem pengikat lilin parafin, polietilina dan asid sterik. 'Hip stem' yang telah diacukan akan direndam didalam heptana pada suhu 60 °C untuk menyingkirkan lilin parafin dan asid sterik. Hasil ujikaji menunjukkan teknik rendaman pelarut dapat menyingkirkan lilin parafin dan asid sterik dalam masa 4 jam dan dapat mengekalkan bentuk 'hip stem' tersebut. Pemerhatian menggunakan SEM menunjukkan lubang liang besar terbentuk dari permukaan ke bahagian tengah semasa proses penyahikatan pelarut dapat juga memendekkan masa penyahikatan disamping dapat memberikan kekuatan jasad perang bagi tujuan pengendalian sampel.

ABSTRACT: Metal Injection Moulding (MIM) has undergone development of various binder systems with the aims of shortening the overall debinding time duration. In this work, the binder system based on wax has been utilised in injection moulding of hip stem using CoCrMo alloy powder. The feedstock consisted of Co-Cr-Mo powder with mean diameter particle size of 16 μm and binder which comprised of paraffin wax, polyethylene and stearic acid. The moulded hip stem was immersed in n-heptane at 60 °C in order to remove the paraffin wax and stearic acid. Results showed that solvent extraction debinding technique allowed complete removal of the paraffin wax and stearic acid from the injection moulded hip stem within 4 hours, without swelling or distortion of the debound part. Scanning Electron Microscopy (SEM) observations have shown that large pores were formed from the surface to the interior of the debound part during the processes. In addition, this technique was found to be suitable to shorten the debinding time, which consequently resulted in a debound part that possesses adequate strength for handling.

In addition, this technique was found to be suitable to shorten the debinding time, which consequently resulted in a rebound part that possesses adequate strength for handling.

Keywords: CoCrMo, MIM, wax, debinding,

INTRODUCTION

Metal Injection Moulding (MIM) is a powder metallurgy process currently used for the production of complicated and near net shape parts of high performance materials (German, 1990). This technique basically combines the advantages of plastic injection molding and the versatility of the conventional powder metallurgy technique. The process overcomes the powder compaction shape limitation, machining cost, isostatic pressing productivity limits, slip casting, and conventional casting defect and tolerance limitations. According to German and Bose (1997), the metal injection moulding (MIM) technology is more complicated than plastic injection moulding, which arises from the need to remove the binder and to densify and strengthen the part. The process is composed of four sequential steps: mixing of the powder and organic binder, injection moulding, debinding (where all binders will be removed) and finally sintering. These processes provide strong inter-particle bonds between powder particles, including removing and reducing the void spaces by means of densification (German and Bose, 1997).

In general, the feedstock is a mixture of metal powder and binder systems. However, the factors determining the feedstock's attributes are the metal powder types, particle sizes and shapes, binder composition, powder-binder ratio and mixing methods. The feedstock designed should be stable as it aged, easy to mould and has uniformity sufficient to provide suitable dimensional control for commercial application. A minimum percentage of binder is needed to fill all the voids between the particles and lubricates particles sliding during moulding. The powder-binder ratio influences the viscosity of the feedstock (German, 2007; Zauner, 2004).

In debinding, the binder must be removed from the moulded specimens. Different debinding methods have been developed for this purpose and can be classified into thermal and solvent debinding. The most commonly used method is the thermal debinding, which is often very slow with the not uncommon debinding durations of several days. While in solvent debinding, significantly faster speed is achieved by dissolving one or more binder components (Hwang, 1996 and 1997). Considerable works have been carried out to improve the classical debinding technologies and to develop alternative binder system with the aims of shortening the overall debinding time duration and minimizing the formation of defects (Angerman, 1992).

Today, the use of Co-Cr-Mo alloy powder for surgical applications is mainly related to orthopedic prostheses for the knee, shoulder, hip and fracture fixation devices. Joint endoprotheses are typically long term implants. Therefore, the applied implant materials must meet the extremely high requirements with regards to biocompatibility with the surrounding body tissue material and corrosion resistance to body fluids (Johnson and Tan, 2000). Materials properties for various Co-Cr-Mo compositions and processing routes are covered by a number of ASTM specifications; such as ASTM F75 for common composition and casting, ASTM F1537 for wrought and forged by ASTM F799. At least three methods of manufacturing are used to make Co-Cr-Mo implants: precise (lost wax) casting, hot forging and powder metallurgy (Marti, 2000). Casting is often selected for surgical implants processing route, while MIM is applied for high volume applications.

The aim of this study is to investigate the feedstock preparation and debinding process mechanism of injection moulding of hip stem using Co-Cr-Mo alloy for medical applications.

MATERIALS AND METHOD

The 90 %-22 μm F75 Co-Cr-Mo powder used in the present study was obtained from Sandvik, UK. The mean particle size distribution was determined using HELOS Particle Size Analysis WINDOX 5 and estimated to be about 9 μm . A scanning electron micrograph showing the powder morphology is indicated is Figure 1. The critical powder loading was determined by the modified American Society for Testing and Materials oil absorption test, ASTM D-28-31. 200 grams of powder were mixed with 8 ml of oleic acid in the mixer. After the mixture become homogenised, 1 ml of oleic acid was added further and the mixture was allowed to become stable for the second time. Every $\frac{1}{2}$ hour, the oleic acid was added until it reaches the maximum torque and the changing torque was recorded. The powder was mixed with a natural paraffin wax, poly ethylene and stearic acid at a solid loading of 65 vol. % for injection moulding (Omar *et al.*, 2013). The mixture of powder and binder was dry mix followed by the entry into the Z-Blade mixer heated up to 160 °C. The mixing was left idled for 1 $\frac{1}{2}$ hour. After the mixing has completed, the heater was shut off and the feedstock was allowed to cool with the mixing blade still in motion. This procedure produces a granulated feedstock.

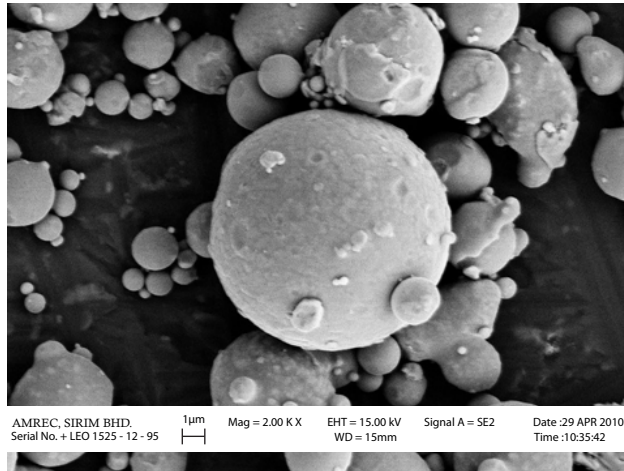


Figure 1. SEM of Co-Cr-Mo alloy powder

The granulated feedstock was then injected into the hip stem prototype using the simple, vertically aligned and pneumatically operated plunger machine, MCP HEK-GMBH. The feedstock was fed into the barrel and then injected through the nozzle in the mould cavity. Prototypes of the hip stems were successfully moulded at the temperature of 200 °C and pressure of 300 bar. The hip stems specimens were then judged and the dimensions measured in order to determine the shrinkage and variation. Next, the hip stems were subjected to solvent extraction of removing the paraffin wax. They were then immersed in n- heptane for 10, 30, 60, 90, 120, 240 and 300 minutes at 60 °C (Omar *et al*, 2003). Subsequently, the debound hip stems were dried at 50 °C for about 2 hours to allow the solvent to evaporate from the pores. Scanning Electron Microscopy (SEM) was used to determine the distribution of powder and binder particles in the specimens before and after the solvent extraction process. The hip-stems which had undergone solvent extraction were subjected to a thermal debinding where the organic binder was completely removed. Then, they were heated with a heating rate of 3-15 °C/minute up to 450 °C and maintained at that temperature for another 2 hours.

RESULTS AND DISCUSSION

Critical Powder Loading Determination

The volume ratio of solid powder to the total volume of powder and binder is defined as the powder loading. In general, it is expected that MIM feedstock has a higher powder loading, which means smaller volume shrinkage of moulded specimen and easier dimensional tolerance control. Nevertheless, too high powder loading is also unacceptable because it will lead to a too high feedstock viscosity and results in failure during injection moulding. Consequently, a suitable powder loading has to be established. A curve of torque evolution for Co-Cr-Mo is depicted in Figure 2. The point of addition of oleic acid can be observed as an increase of torque reading as shown in Figure 2. The shape of the torque curve is typical of the mixing done with sequential addition of oleic acid in metal powder.

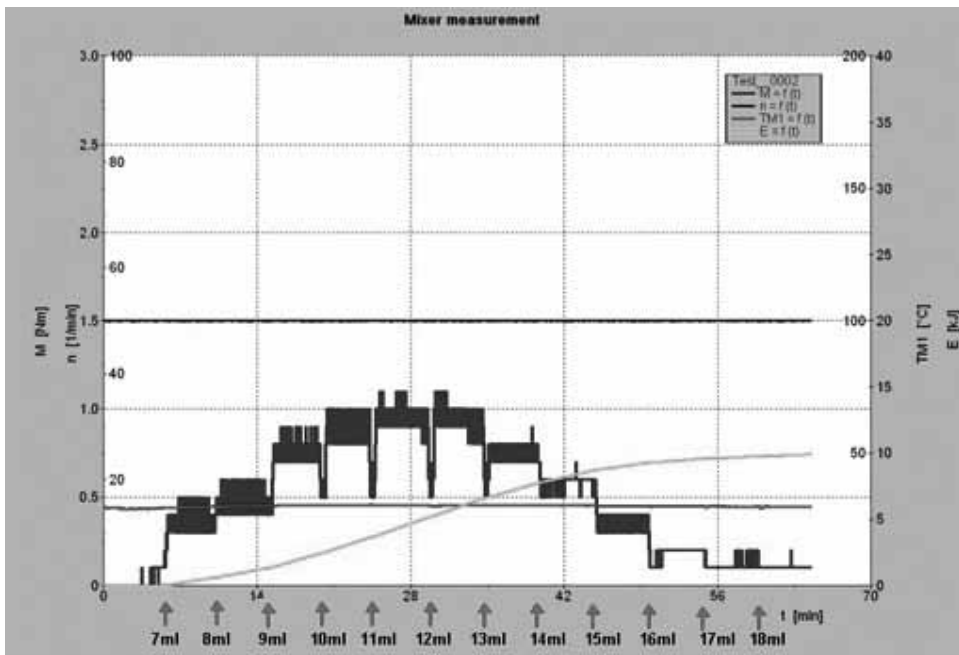


Figure 2. The torque curve for the determination of powder loading

At the beginning, the torque was zero but addition of 7 ml of oleic acid increased the torque rapidly and reached a peak of 0.5 Nm. Followed by the reduction to a steady value greater than zero. The irregular peaks indicate the melting and the consolidation processes. Once the torque reaches a steady state that indicates the uniformity of the mix viscosity, no additional mixing takes place. Further addition of 1 ml oleic acid (a total addition of 8 ml) caused the torque to increase again and reached a value of 0.6 Nm. However, after adding 6 ml of oleic acid (a total addition of 13 ml), the torque decreased to 0.8 Nm and continued to decrease with more

oleic acid additions. Nevertheless, after an addition of 9 ml (a total addition of 16 ml of oleic acid), the torque reached its final value of 0.2 Nm.

The different torque value observed with the addition of oleic acid may be attributed to either, miscibility between the powder and the amount of oleic acid in the melt, or shear effect due to the increased amount of mass in the compounder. Both reasons seem plausible. On one side, the miscibility in the melt would imply colligative effect of the stearic acid melting temperature, while on the other side, more heat dissipation increases the mixing temperature causing melting to occur by heat transfer.

Figure 2 also reveals that the torque attained the highest value of 1.0 Nm after addition of 12 ml oleic acid. Although the torque decreased after an addition of 13 ml stearic acid, the value of torque was still considered to be high (0.8 Nm). However, with an addition of 16 ml, the torque value decreased to its final value of 0.2 Nm. It is also apparent that the activation energy (E) is increased upon the addition of 15 ml oleic acid and achieved a constant value of 10 kJ. This result confirmed the effect of temperature on the viscosity of the continuous phase as the dominant factor.

The optimum oleic acid content is the amount added at the maximum value of the torque before it reached the lowest value and this is considered as the critical powder volume concentration (CPVC) value. This CPVC is the point where the particles are tightly packed and assuming all voids between the particles are filled with binder. Equation 1 was adopted to obtain the correlation between the volume of oleic acid and torque value and the results are as shown in Table 1. The theoretical density of Co-Cr-Mo is 8.2 g/cm³.

$$CPVC = 100 \times \frac{V_f}{(V_f + V_o)}$$

where; V_f = volume of powder (cm³) (1)

$$= \frac{\text{Actual weight of powder (g)}}{\text{Theoretical density of powder (g/cm}_3\text{)}}$$

V_o = volume of oleic acid

Table 1. Correlation volume of oleic acid and volume fraction of powder

volume of oleic acid (cm³)	volume fraction of powder (%)
7	83.94
8	82.06
9	80.26
10	78.54
11	76.89
12	75.3
13	73.79
14	72.33
15	70.92
16	69.58
17	68.28
18	67.03

The results obtained showed that the CPVC of Co-Cr-Mo is 70.42 vol.%. As the optimum powder loading for MIM is usually in the range of 2 % to 5 % less than critical powder loading (German and Bose, 1997), hence the selection of the powder volume fraction falls in the range of 67 vol. % to 65 vol. %. Nevertheless, it depends on many other factors such as powder size, shape and type of binder used. In this present study, further investigation will be based on the 65 vol. % powder loading.

Injection Moulding of the Feedstock

The detail of the processing parameters during injection moulding of the hip stem is tabulated in Table 2. All prototypes were in good condition and free from normal defects such as short moulding, obvious flashes at the parting surfaces and obvious separation between the powder and binder.

Table 2. Moulding parameters (optimum) for producing hip stem prototype (65 vol.%)

Moulding parameters	Value
Injection temperature	200 - 210oC
Injection pressure	300 bar
Cycle time	15-20 sec
Mould temperature	Room temperature

Figure 3 shows the prototype of injection moulded hip stem. The moulded part is sufficiently hardened at room temperature in the mould and can be removed from the mould cavity after 20 seconds. The moulded part which is called the 'green body' has sufficient strength to be handled and was produced without any significant defects such as short shot, flashes and binder separation. Evaluation

on the injection moulding process at various temperatures revealed that higher moulding temperatures resulted in better flow of the feedstock during the moulding process.



Figure 3. Prototype of injection moulded hip stem

Solvent Extraction Process

Figure 4 depicts the effect of leaching time on the rate of binder extraction at 60 °C. It shows that the rate of extraction increased with the increasing solvent extraction time. For the first 2 hours, the slope of the curve is steep, which shows that the removal rate of paraffin wax was fast due to more interconnected pore channels through which dissolved solution can diffuse to the surface. Moreover, the solvent leach the soluble binder component with ease, since the binder phase is on or near the compact surface, ensuring a faster debinding rate.

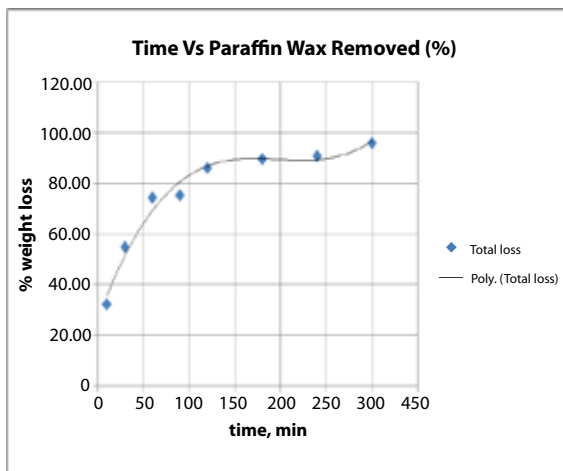


Figure 4. The effect of leaching time on wax removal at 60°C

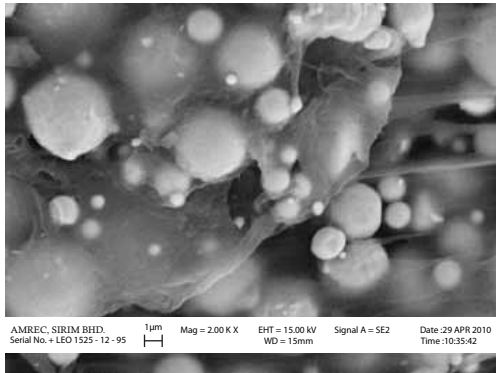
Dissolution is the rate-determining in the first step of solvent extraction. After 2 hours, the slope of the curve is slightly horizontal which means that the removal rate of the paraffin wax had slow down. As debinding proceeds, the core portion of the compact containing binder recedes from the surface, making diffusion as

the rate-determining step. The removal rate of paraffin wax becomes smaller as the solvent extraction time increases owing to the increased length of the porous channels through which the polymer diffuses out.

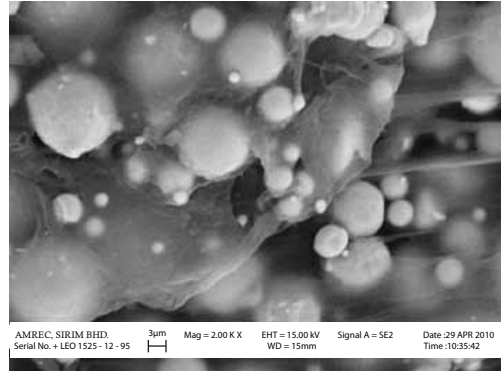
SEM Observation During Solvent Extraction

The binder distributions and evaluation of interconnected porosity with time during solvent extraction in n-heptane were observed using Scanning Electron Microscopy (SEM). Different areas of the debound specimens were examined, including the outer and the central regions of fractured surface in order to monitor the progress of the solvent extraction process. Figure 5 displays the formation of the open pore channels as the paraffin wax was extracted from the moulded specimens at different time, as the specimens were immersed in the n-heptane bath at 60 °C. As the time increased, the weight loss of paraffin wax increased and the pore channel enlarged. The SEM images of the debound specimen with extracting time of 10 minutes (Figure 5 (a)) showing that there are still much amount of binder left interstices between the powder particles while Figure 5 (d) indicates most of the paraffin wax was removed after 240 minutes. It can be clearly seen that a network of porous polyethylene ligaments remained, binding and holding the powder particles together to provide the moulding with sufficient brown strength to be handled.

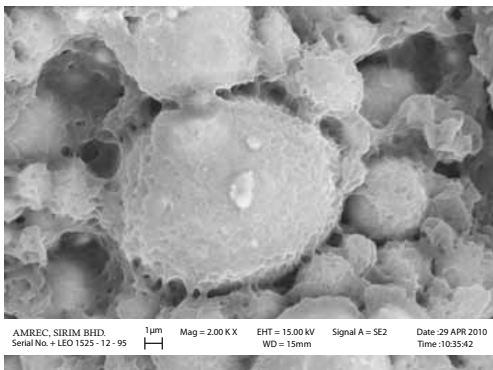
The removal process of paraffin wax in moulded specimens can be postulated as a combination of two processes consisting of dissolution and diffusion. Initially, the solvent penetrates the binder phase and dissolves the soluble binder components and creates porous surface. The solvent then gets into the pores by capillary action. This is followed by the diffusion of dissolved polymeric substances out of the green specimens. The dissolved component diffuses through the porous paths among the powder particles and leaves the specimens. Since the diffusion is easier and solvent is in direct contact with the polymer, the dissolution of the paraffin wax is the rate-limiting step in the beginning of the solvent extraction process. As the process proceeds, a longer diffusion distance through porous channels formed after initial debinding slowing down the process and diffusion becomes rate-determining step (Omar, 1999; Omar *et al.*, 2011; Omar *et al.*, 2012; Omar, 2013).



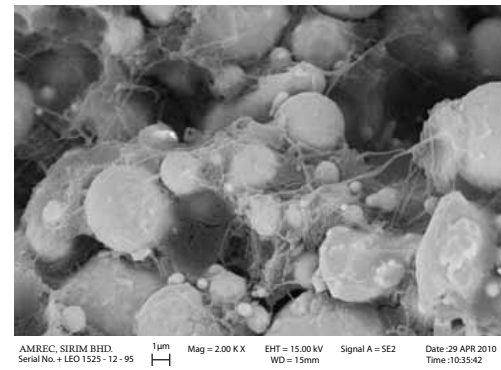
a) 10 minutes



b) 60 minutes



c) 150 minutes



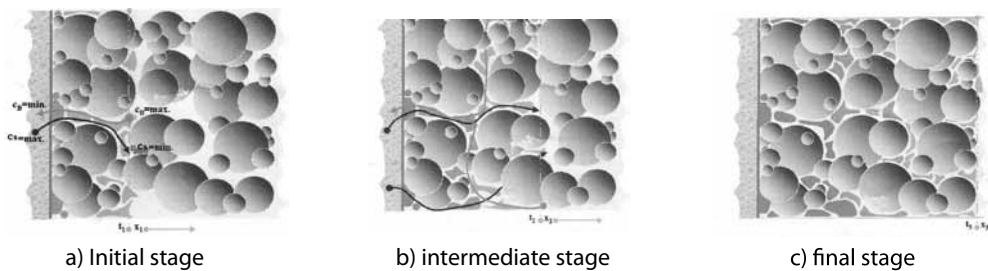
d) 240 minutes

Figure 5(a-d): Formation of open pore channels during extraction

Proposed Schematic Mechanism of Binder Removal During Solvent Extraction Process

During solvent extraction, the removal process of soluble binder in green specimens can be postulated as a combination of two processes, dissolution and diffusion as illustrated in Figure 6. After a short time (t_1), as the moulded specimens were immersed in the solvent bath, the n-heptane penetrates into the green microstructure and dissolves the soluble binder (x_1). The dissolved binder (CB) moves out of the structure into the direction of the n-heptane bath, and vice versa, n-heptane (CS) migrates from the bath to the place of chemical reactions as illustrated in Figure 6(a).

Figure 6 (b) shows the schematic of binder distributions at the intermediate stage of solvent debinding. The solution reactions continue by migrating as a front (x_2) into the center of the specimens. After the completion of the solution reaction (t_2), an open porosity remains in the green specimen which serves as diffusion path. As the debinding time continued to 3 and 5 hours, the pore size and pore volume increased and the distribution of pores broadened obviously. After having reached the geometric centre of the component (x_3), the solution reaction (t_3) ends as illustrated in Figure 6(c). The matrix of insoluble binder parts gives the large component stability and the pore channels could serve as escape paths for decomposed gas during subsequent thermal debinding for insoluble binder.

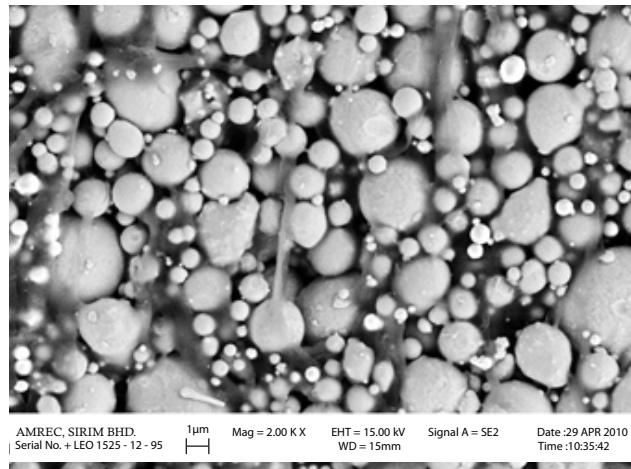


a) Initial stage b) intermediate stage c) final stage
 Figure 6. Scanning electron micrograph of thermal pyrolysis samples at 200 °C and 450 °C

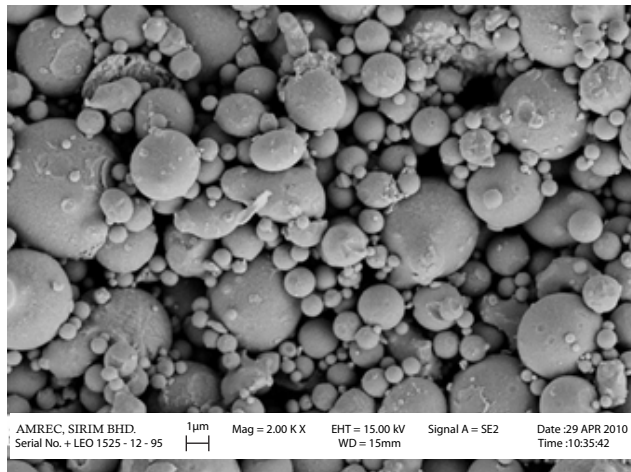
THERMAL PYROLYSIS PROCESS

SEM Observation During Thermal Pyrolysis

After the paraffin wax binder has been removed by solvent extraction, the remaining binder of polyethylene was removed thermally. Figure 7 shows the micrograph of the part which had been debound in solvent and thermally pyrolysed at different temperatures with a heating rate of 5 °C/minute and holding time of 1 hour. These micrographs illustrate the progressive removal of the polyethylene with increasing pyrolysis temperature.



a) 200 °C



b) 450 °C

Figure 7. Scanning electron micrograph of thermal pyrolysis samples at 200 °C and 450 °C

A small bonding which is believed to be polyethylene, still can be seen especially at the powder-powder contact region as shown in Figure 7 (a). After the temperature reached 450 °C, it was observed that the removal was completed, although some small proportion of the binder still remained as shown in Figure 7 (b). Moreover, the binder at contact points provide enough capillary forces to hold particles together.

Proposed Schematic Mechanism of Binder Removal During Thermal Pyrolysis Process

Figure 8 illustrates the schematic diagram of binder distribution during thermal pyrolysis. As moulded hip stem were heated, the residual binder decomposes into low molecular weight components. Since at this stage, there is porosity in the part according to the dissolved binder during solvent extraction, the decomposed gas can escape from the centre into the ambient atmosphere without causing pressure build-up in the interior as illustrated in Figure 8 (a).

As debinding advances into the final stage of thermal debinding, all binders in the inter-particle voids were completely burnt out except at the contact areas between powders as illustrated in Figure 8 (b). This binder formed pendular bonds and held particles together while debinding continued.

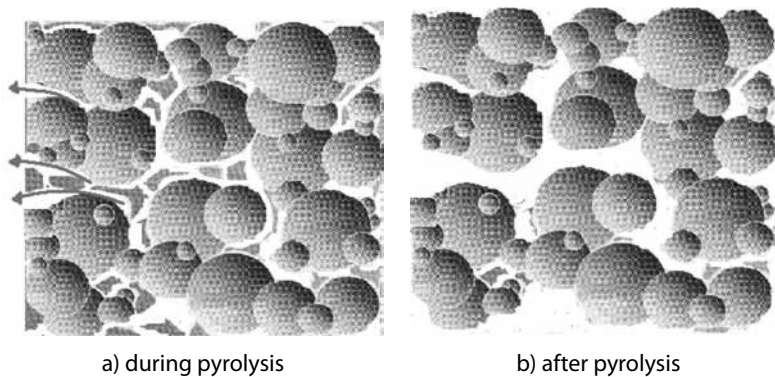


Figure 8. The proposed schematic mechanism of binder distribution;
(a) during thermal pyrolysis and (b) after thermal pyrolysis process (Omar,2006)

As this force held particles together, sintering proceeded concurrently at the contact points where the driving force was high due to the curvature small radius. Thus, the binders at contact points were all gone; the specimens could still retain the shape because slight sintering had occurred.

CONCLUSION

This study shows that a critical powder volume concentration (CPVP) for Co-Cr-Mo alloy powder was 70.15 vol.%. The prototype of hip stem Co-Cr-Mo alloy powder was successfully injection moulded using the wax based binder at a temperature of 200-210 °C with maximum injection pressure of 300 bar. The moulded parts were in good condition and free from normal defects such as short moulding, flashing and parting surface. The major steps in the removal of binder from the moulded hip stem Co-Cr-Mo alloy powder can be summarized as follows:

1. The removal of the major fraction of the binder (paraffin wax) by solvent extraction resulting in the formation of a network of open pore channels in the body.
2. Thermal pyrolysis of the remaining binder (polyethylene and stearic acid) formed a monomer in a form of a gas at the burn out temperatures.
3. It is shown that the solvent debinding process coupled with thermal removal of the remaining binder phase was found to be easier and less tedious than the process of partial wick debinding and thermal degradation of the binder phase.

ACKNOWLEDGEMENT

The authors wish to thank MOSTI for financial support under Science Fund grant no. 03-03-02-SF0247 and SIRIM Bhd.

REFERENCES

- Angerman, H.H., Yang, F. K., & Biest, O.V.D. (1992). Removal of low molecular weight component during thermal debinding of powder compacts. *Journal of Material Science*, 27, pp 2534-2538.
- German, R.M. (1990). Powder Injection Moulding, MPIF, Princeton, NY, pp 1-120
- German, R.M. and Bose, A. (1997). Injection Molding Of Metals and Ceramic. Metal Powder Industries Federation, Princeton, New Jersey, pp 1-38
- German, R.M. (2007). Powders, binders and feedstock for powder injection moulding. *Powder Injection Moulding International*, 1(1), 34-39.
- Hwang, K.S., & Hsieh, Y.M. (1996). Comparative study of pore structure evolution during solvent and thermal debinding of powder injection molded parts. *Metallurgical and Materials Transactions A*, 27A, 245-252.
- Hwang, K. S., Lin, H. K., & Lee, S. L. (1997). Thermal, solvent and vacuum debinding mechanism of PIM compacts. *Material and Manufacturing Process*, 12(4), 593-608.
- Johnson, J.L and Tan, K.L. (2000). Processing of MIM CO-28Cr-6Mo,. *Advances in Powder Metallurgy* : pp 13-19
- Kim, S.W., Lee, H-W., Song, H., & Kim, B.H. (1996). Pore structure evolution during solvent extraction and wicking. *Ceramic International*, 22, 7-14.
- Marti, A., (2000). Cobalt Based Alloys Used in Bone Surgery. *Int. J. Care Injured*, 31, pp: 18-21
- Mohd Afian Omar, (2013). Metal Injection Moulding Process: An Advanced Processing Technology , *Metal Injection Moulding of Implants Materials* , Chapter 1, ISBN 978-967-11588-1-4, pp: 1-16
- Omar, M.A. (1999),PhD Thesis, University of Sheffield

Omar, M.A., Ibrahim, R., Sidik, M.I., Mustapha, M., & Mohamad, M. (2003). Rapid debinding of 316L stainless steel injection moulding component. *Journal of Materials Processing Technology*, 140, 397-400.

Omar, M.A., Ibrahim, R. & Mohamad, M. (2006, Feb). *Environmental friendly binder system for powder injection moulding process*. Exhibition presented at the Malaysia Technology Expo (MTE) 2006, PWTC, Kuala Lumpur, Malaysia

Omar, M.A, Abdullah, N., Roslani, N., Zainon, M.N., and Meh,B. (2011). Development of injection moulded Co-Cr-Mo alloy powder using palm based binder. *Solid State Science and Technology*, Vol. 19, No2, pp: 61-69

Omar, M.A., (2013). Development of injection moulded CoCrMo alloy powder for orthopaedic applications. *Microsom* , June 2013, pp 5-8

Omar, M.A., Ibrahim, R., Sidik, M.I., Mustapha, M., Mohamad, M., (2003). Rapid Debinding of 316L Stainless Steel Injection Moulding Component, *Journal of Materials Processing Technology*, 140, pp: 397-400.

Schwartz, S., Quirnbach, P., & Kraus, M. (2002). Solvent debinding technology for a continues 316L MIM production. *Advances in Powder Metallurgy and Particulate Materials*, 147-155.

Zauner, R., Binet, C., Heaney, D.F., & Piemme, J. (2004). Variability of feedstock viscosity and its correlation with dimensional variability of green powder injection moulded component. *Powder Metallurgy*, 47(1), 1-6.